Ceramics International **24** (1998) 265–272

PII: S0272-8842(97)00008-4
0272-8842/98 $19.00+.00

The Growth and Characteristics of CVD SiC–TiC In-situ Composites

Tain-Tsair Lin,* Jung-Fang Chang & Min-Hsiung Hon

Department of Materials Science and Engineering, National Cheng Kung University, Tainan, 70101, Taiwan

(Received 1 August 1996; accepted 30 September 1996)

Abstract: SiC–TiC in-situ composites have been synthesized by low pressure chemical vapour deposition on graphite with $SiCl_4$, $TiCl_4$ C_3H_8 and H_2 reaction gases to improve the toughness of SiC–TiC ceramics. The composite was deposited at various temperatures (1500~1600°C), total pressure (40~300 torr) and reactant concentrations. The microstructure was investigated by scanning electron microscopy, optical microscopy and transmission electron microscopy. The morphologies of facet structure, nodular structure and dendrite structure appear depending on the experimental conditions. A dense SiC–TiC deposit without porosity was obtained with a maximum growth rate of 1.6 mm h^{-1} at $C_3H_8 = 25\,cm^3$ min^{-1} and 200 torr. Only β-SiC and TiC phases have been identified in the composite with a dramatic change of the composition at the interface of SiC and TiC grains. The fracture toughness (K_{Ic}) determined by the indentation method exhibits a value as high as 5.9 MPa $m^{1/2}$ that could be obtained by deposition at low pressure and low C_3H_8 concentration. Cracks propagate with more deflection in the SiC–TiC composites than in monolithic SiC. The result is due to existing severe strain at the SiC–TiC interface observed by transmission electron microscopy.

1 INTRODUCTION

Silicon carbide has very excellent mechanical, physical and chemical properties, such as high temperature strength, high hardness, oxidation resistance, chemical inertness and so on. It is currently used in wear-resistant and structural applications, but the moderate fracture toughness values (3~4 MPa $m^{1/2}$) limit its applications. Improvement of SiC fracture toughness is an important task for scientists and engineers. Over the last decade, silicon carbide matrix composites incorporating whiskers,[1,2] fibres[3,4] and particles,[5,6] have been reported for improving SiC toughness.

A few years ago, a number of researchers concentrated their efforts on improving the SiC toughness with TiC dispersed by a chemical vapour deposition (CVD) method. Theoretically dense, clean grain boundary, homogeneous and multiphase materials could be obtained at reduced processing temperature. Nickel *et al.*[7] first developed a CVD phase diagram of multiphase domains from the $TiCl_4$–$SiCl_4$–CCl_4–H_2 system at 1200°C and 760 torr (1 torr = 0.133 KPa). The growth mechanisms and crystal orientation relationships between the SiC matrix and dispersed phases are also described. Goto and Hirai[8,9] reported that SiC–TiC in-situ composites with a porous and granular structure contained free carbon, $TiSi_2$ and Ti_3SiC_2 from $TiCl_4$–$SiCl_4$–C_3H_8–H_2 system at 1300~1600°C and 30~300 torr. The fine SiC particles dispersed uniformly in the TiC matrix with a dense platelike structure. The toughness is higher than 10 MPa $m^{1/2}$. Kawai *et al.*[10,11] fabricated CVD SiC–TiC composites from the $SiCl_4$–$TiCl_4$–CH_4–H_2 system at 1350°C and 60 torr. The K_{Ic} values are about 3~4 times as large as for monolithic SiC or TiC and twice of sintered TiC–SiC composites. Touanen *et al.*[12,13] reported SiC–TiC multiphase materials

*To whom correspondence should be addressed.

deposited from a SiH_2Cl_2–C_4H_{10}–$TiCl_4$–H_2 system at 950~1150°C and 760 torr. The nanocomposition always contains amorphous carbon in SiC matrix with Vickers microhardness of 1500 kg mm^{-2}. Stinton[14] investigated several ceramic–ceramic composites by CVD techniques. The fracture toughness of SiC–$TiSi_2$ composites was increased to 5.5 MPam$^{1/2}$ using a precursor of CH_3SiCl_3–$TiCl_4$–H_2 at 1700°C and 7.6~760 torr.

A $SiCl_4$–C_3H_8–H_2 system has been reported by Parretta *et al.*[15] for SiC deposition and the precursor had a fastest deposition rate than other reaction sources. In the present work, SiC–TiC in-situ composites are prepared by CVD using a precursor $SiCl_4$–$TiCl_4$–C_3H_8–H_2 system. The main purposes are to improve toughness by changing the process parameters, such as deposition temperature, total pressure, C_3H_8 flow rate and $TiCl_4$/($TiCl_4$ + $SiCl_4$) ratio.

2 EXPERIMENTAL PROCEDURE

The SiC–TiC deposits were prepared on graphite substrate by CVD under reduced pressure (40~300 torr) and 1500~1600°C in a 300 mm in diameter and 400 mm in length cold wall reactor (Fig. 1). The temperature was measured with an optical pyrometer for holding constant emission coefficient of graphite. The precursors, $SiCl_4$,$TiCl_4$ and C_3H_8, were the source of silicon, titanium and carbon, respectively, with hydrogen as a carrier gas. The flow rates of the liquid sources, $SiCl_4$ and $TiCl_4$, were controlled by H_2 bubbling through the saturated thermal baths. The detailed experimental parameters are listed in Table 1. The graphite substrates were ground to #1200, then cleaned with acetone in an ultra sonic machine, and pre-heated near the deposition temperature to avoid the absorption of impurity and humidity before deposition. The surface morphology and crystal structure were determined by scanning electron microscopy (SEM) and X-ray diffraction respectively. The distribution of dispersed TiC phase in SiC matrix was investigated by optical microscopy (OM) and transmission electron microscopy (TEM). The microindentation technique with 300 g load was used to measure the Vickers' hardness to estimate the K_{Ic} from the crack length referring to Niihara's report.[16]

3 RESULTS AND DISCUSSION

3.1 Growth characteristics

Figure 2 shows the variations of the SEM morphology of SiC–TiC composite deposited at 1500°C and the flow rate of C_3H_8 = 25 cm^3 min^{-1} at various pressures. The morphology changes gradually from a fine grain to a strong facet. The grain size increases with increasing gas pressure resulting from a high boundary concentration near the substrate surface at high pressure. The striations observed at the surface result from multiple twins which appear more evident with increasing pressure. A twin is a significant site for enhancing the growth propagation. In a CVD process, there exists a boundary layer above the substrate. In general the transport of reactant through the boundary layer to the substrate, adsorption of reactants at the substrate and chemical reactions on the substrate occur, then the products diffuse out from the substrate through the boundary layer. Therefore, at 1500°C deposition temperature, the growth kinetics is controlled by diffusion, however in this situation a faceted morphology is easily

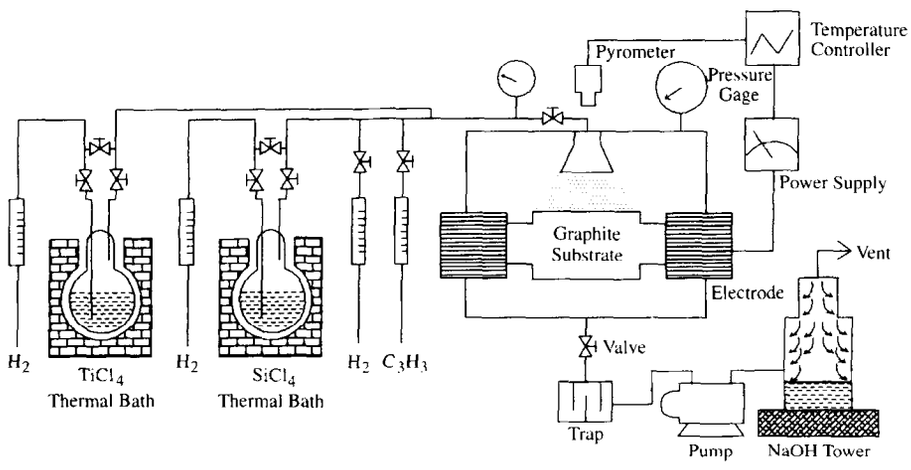

Fig. 1. Schematic diagram of CVD SiC–TiC deposition system.

Table 1. The experimental parameters used for SiC–TiC composite deposition

Total pressure	40~300 torr
Deposition temperature	1500~1600°C
Deposition time	30 min
Flow rate of H_2	3000 cm^3 min^{-1}
Flow rate of C_3H_8	25~35 cm^3 min^{-1}
Flow rate of $TiCl_4$	105~165 cm^3 min^{-1}
Flow rate of $SiCl_4$	41.2~130 cm^3 min^{-1}

developed due to a higher surface activity and a low supersaturation of species.

When C_3H_8 inlet concentration increases to 35 cm^3 min^{-1}, the surface morphology changes from fine facet formed at 40 torr to nodule at 100 torr and cauliflower at 300 torr as shown in Fig. 3. The morphology change of the deposited layers may be due to the contribution of homogeneous and secondary surface nucleation. In the pressure range of 100 to 300 torr, the growth kinetic of the film is diffusion controlled. The increment of total pressure favours a secondary nucleation resulting in a nodular structure (Figs 3(b)–(d)). At a total pressure of 40 torr, the limited residence time of the precursor and the carrier gas in the reaction chamber restricts the nucleation process whereas favors crystal growth coming to a faceted structure (Fig. 3(a)). The dependence of growth rate on the gas pressure for different C_3H_8 concentrations is shown in Fig. 4. The growth rate increases with increasing pressure to reach a maximum. Then the growth rate decreases with increasing pressure due to particles formed by homogeneous nucleation in the gas phase being taken away by the gas stream. In fact this is easier to occur at a higher deposition pressure and a higher C_3H_8 concentration such as at pressure higher than 100 torr for C_3H_8 = 25 cm^3 min^{-1} and 200 torr for C_3H_8 = 35 cm^3 min^{-1}. Although the growth rate is very high reaching maximum values of 1.1 mm h^{-1} and 1.6 mm h^{-1} for 25 cm^3 min^{-1} and 35 cm^3 min^{-1} C_3H_8, respectively, all the deposits are fully dense as observed on the polished specimen.

The result of XRD analyses of deposits formed at different C_3H_8 flow rates are shown in Fig. 5. Owing to the similar crystal structure for the SiC and TiC composites (Zinc blend structure for SiC and rock salt structure for TiC) with a close lattice constant (a = 0.4358 nm for SiC and 0.4327 nm for TiC), it is difficult to distinguish the peaks in the spectra of SiC–TiC composite for each other, especially for the lattice being distorted by stresses induced in cooling after deposition and with a strong preferred orientation deriving from the CVD process. The (220) peak in Fig. 5(a) derives

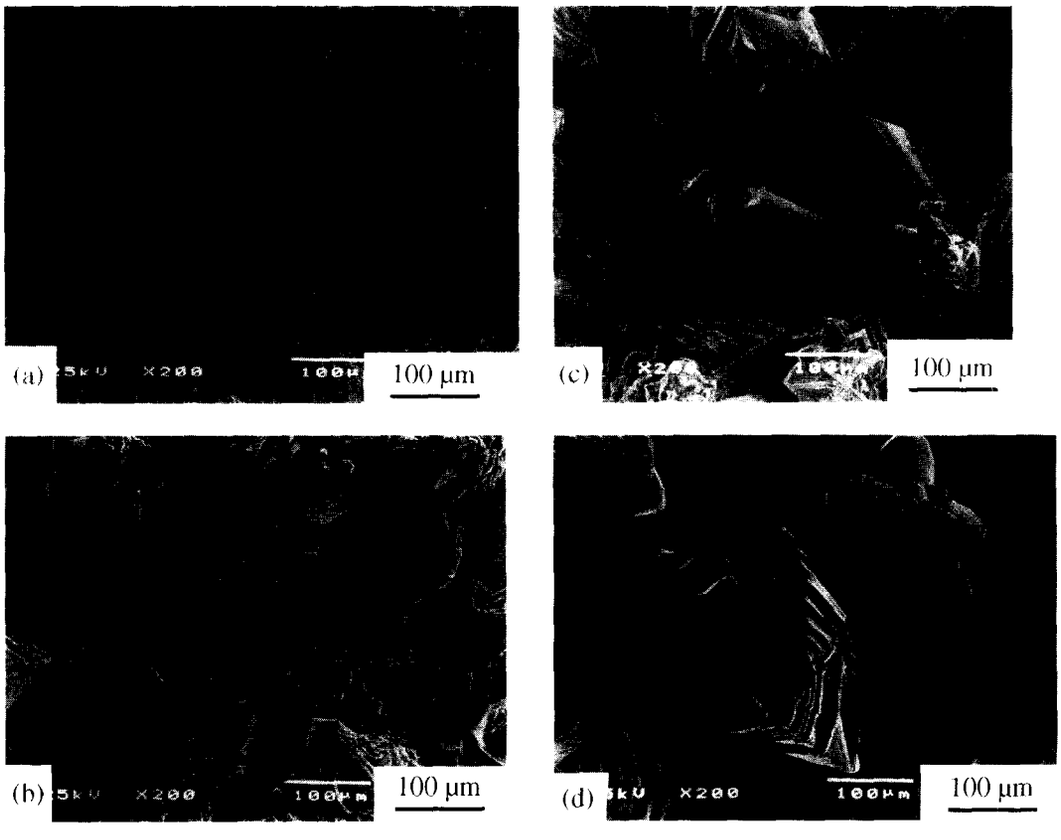

Fig. 2. SEM surface morphology of specimens deposited at C_3H_8 = 25 cm^3 min^{-1} and pressures of (a) 40 torr; (b) 100 torr; (c) 200 torr; (d) 300 torr (1500°C, $TiCl_4$ = 105 cm^3 min^{-1}, $SiCl_4$ = 130 cm^3 min^{-1} and H_2 = 3000 cm^3 min^{-1}).

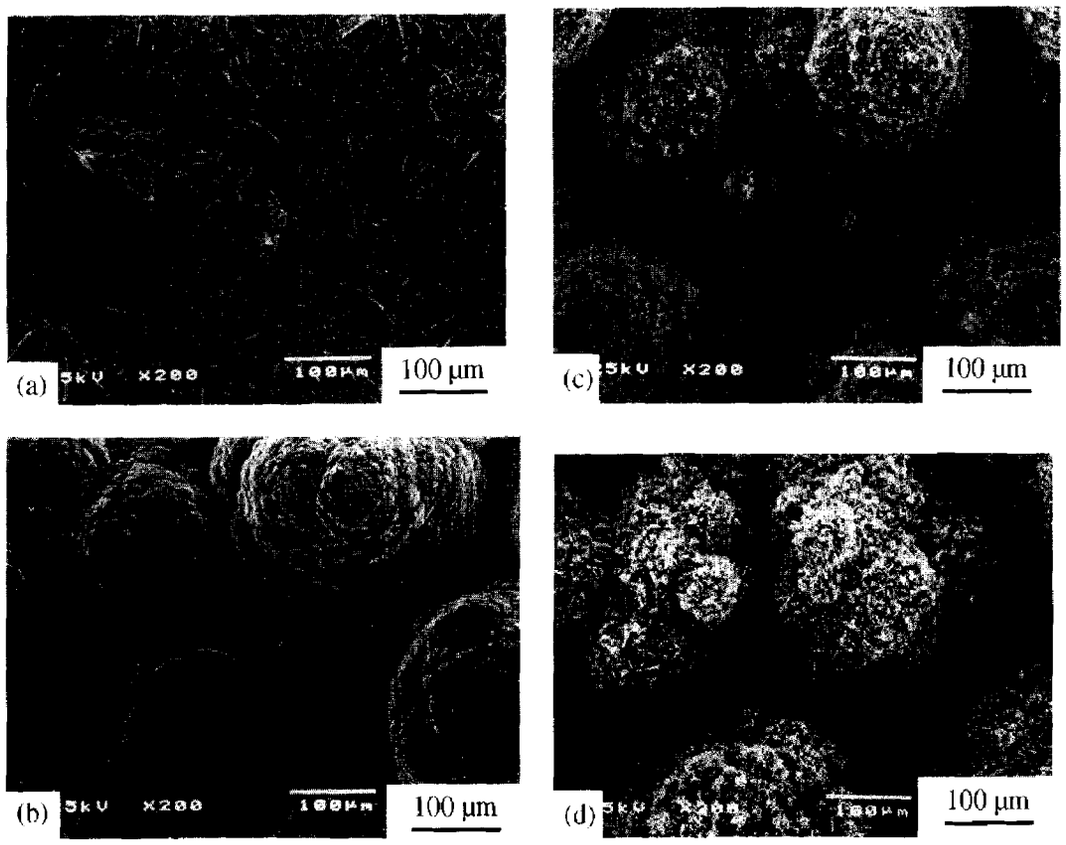

Fig. 3. SEM surface morphology of specimens deposited at $C_3H_8 = 35\,cm^3\ min^{-1}$ and pressures of (a) 40 torr; (b) 100 torr; (c) 200 torr; (d) 300 torr (1500°C, $TiCl_4 = 105\,cm^3\ min^{-1}$, $SiCl_4 = 130\,cm^3\ min^{-1}$ and $H_2 = 3000\,cm^3\ min^{-1}$).

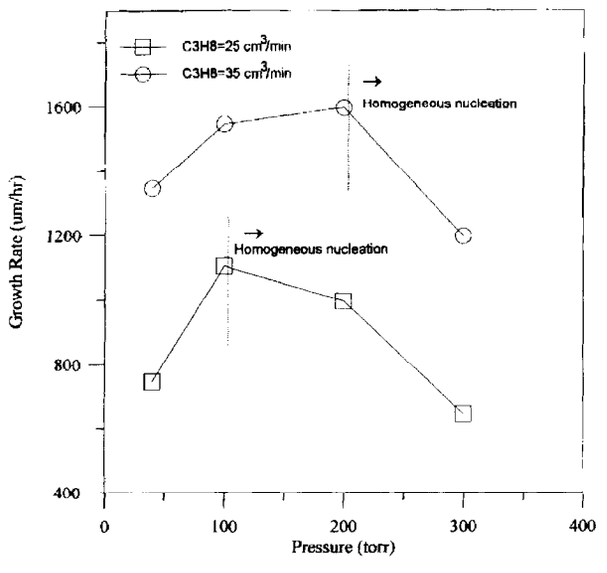

Fig. 4. Growth rate dependence of SiC–TiC composite on the deposition pressure at (□) $C_3H_8 = 25\,cm^3\ min^{-1}$; (○) $C_3H_8 = 35\,cm^3\ min^{-1}$.

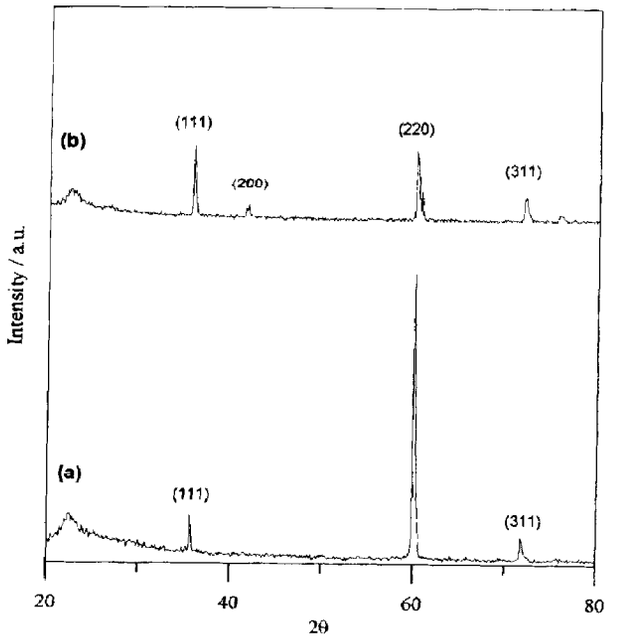

Fig. 5. XRD patterns of CVD SiC TiC composite deposited at (a) $C_3H_8 = 25\,cm^3\ min^{-1}$; (b) $C_3H_8 = 35\,cm^3\ min^{-1}$.

from the preferred orientation of CVD SiC deposited at high temperature while the presence of [200] suggests the existence of TiC phase. Hence increase of the (200) peak intensity for the film deposited at $C_3H_8 = 35\,cm^3\ min^{-1}$ implies an increase of the TiC component in the composite.

3.2 Microstructure and composition analysis

The optical micrographs shown in Fig. 6(a)–(d) are the top and cross-section views of the polished SiC–TiC composite deposited at $C_3H_8 = 25\,cm^3\ min^{-1}$ and $C_3H_8 = 35\,cm^3\ min^{-1}$, respectively. The

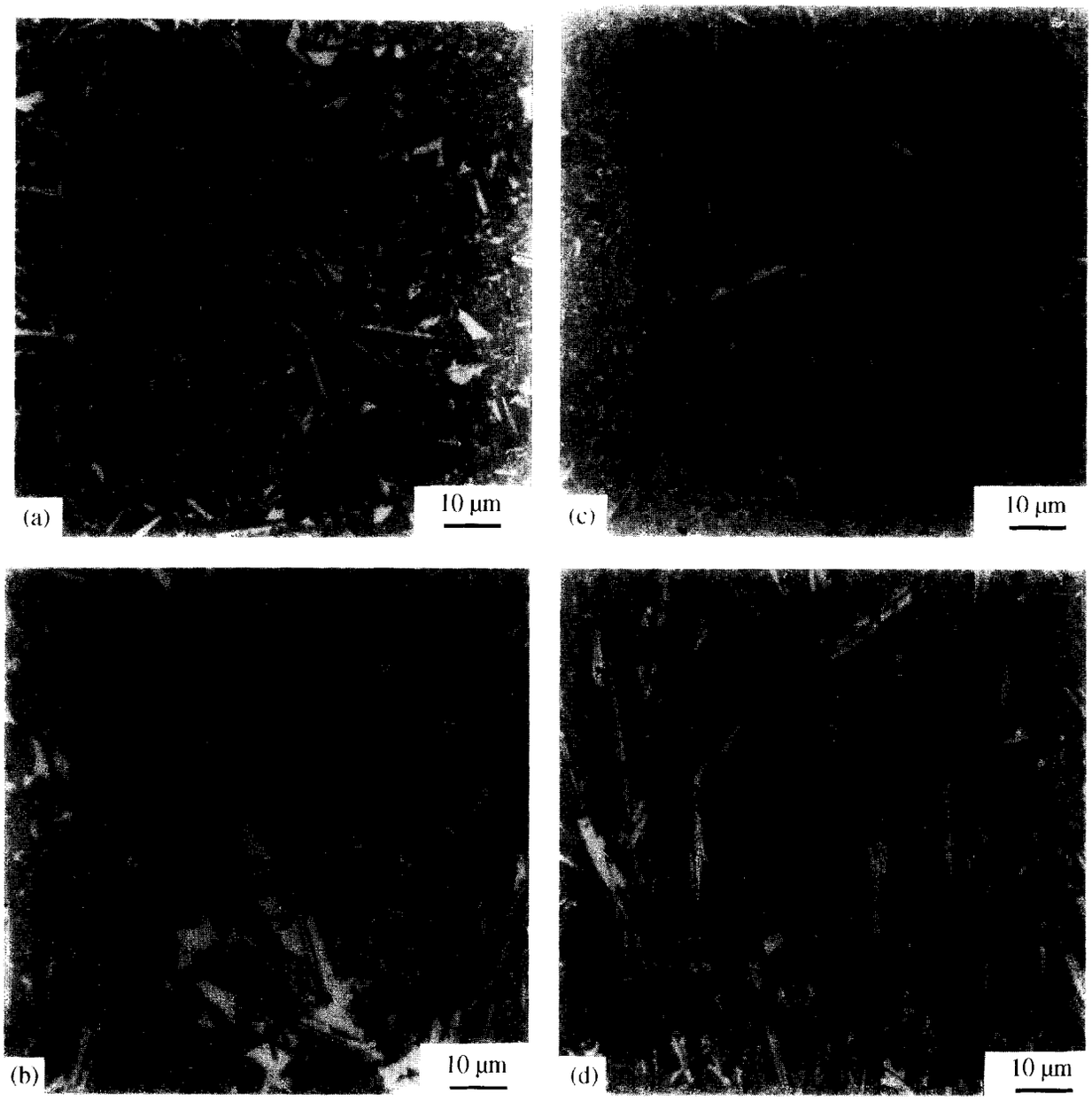

Fig. 6. Microstructures of the SiC–TiC composite for (a) topic view; (b) cross-section deposited at $C_3H_8 = 35\,cm^3\ min^{-1}$ and (c) topic view; (d) cross-section deposited at $C_3H_8 = 35\,cm^3\ min^{-1}$.

white plate is TiC and the grey matrix is SiC. The white region of TiC in Fig. 6(a) deposited at $C_3H_8 = 25\,cm^3\ min^{-1}$, is less than that in Fig. 6(c) deposited at $C_3H_8 = 35\,cm^3\ min^{-1}$, which agrees with the postulation of [200] peak intensity in Fig. 5(b). The reason is that increasing C_3H_8 concentration in the gas source leads to the TiC formation in the deposit. The TiC uniformly distributes in the SiC matrix with a columnar structure, whereas near the substrate surface the various fine grain structure observed may be due to an unstable growing at the beginning of deposition. A series of polished samples in Fig. 2 show the TiC dendrite rise increase with increasing gas pressure.

A typical microstructure with facet morphology deposited at 1600°C is shown in Fig. 7(a). The dendrite structure shown in Fig. 7(c) is normal to the substrate. When the ratio of $TiCl_4/(TiCl_4 + SiCl_4)$ is increased to 8.0, the TiC fraction increases, whereas the facet structure disappears and the grain size of dendrites decrease as shown in Fig. 8.

The composition of SiC–TiC composite has been analyzed by WDX using CVD monoclinic SiC and TiC as a standard. The results show that the TiC plate and SiC matrix are almost pure. The line scanning profile in Fig. 9 shows that the titanium dominates in white region and the silicon dominates in grey matrix. The composition changes suddenly at the interface of SiC–TiC, i.e. without composition gradient.

The TEM image of SiC–TiC specimen in Fig. 10 shows the darker TiC phase and lighter SiC grains

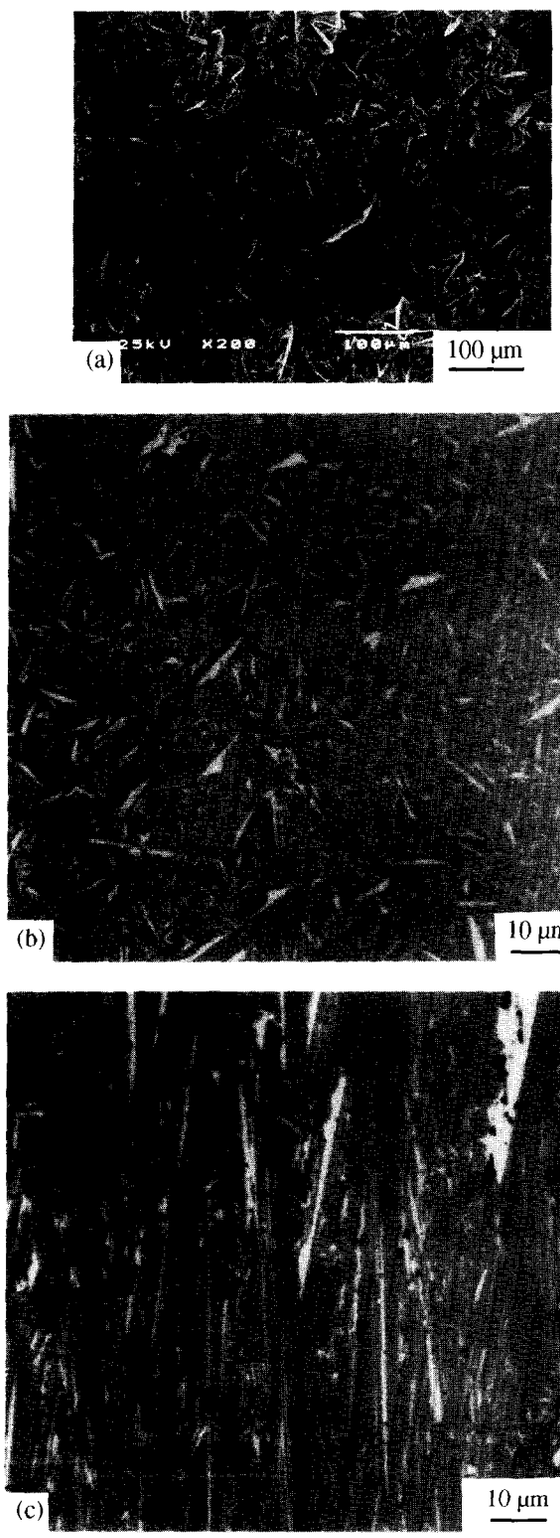

Fig. 7. Microstructure of SiC–TiC composite deposited at 1600°C for (a) SEM morphology; (b) polished topic view; (c) polished cross-section ($C_3H_8 = 25$ cc min^{-1}, $TiCl_4 = 105$ cm^3 min^{-1}, $SiCl_4 = 130$ cm^3 min^{-1}, $H_2 = 3000$ cm^3 min^{-1} and 100 torr).

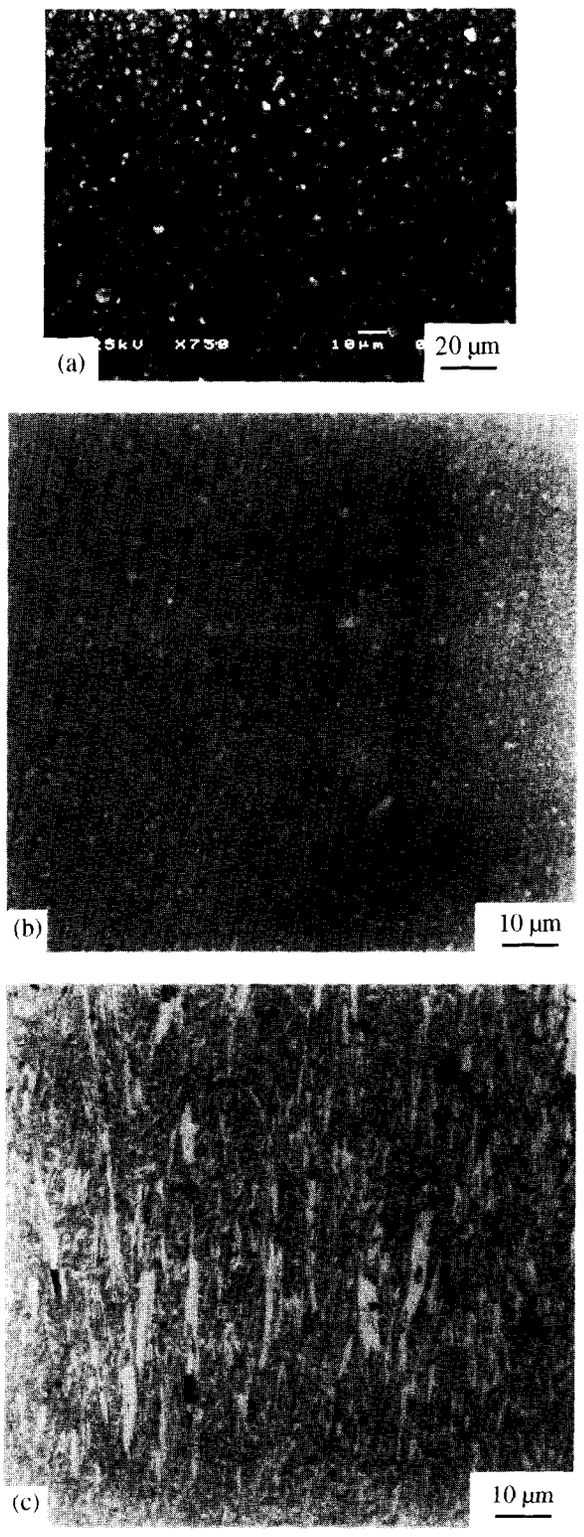

Fig. 8. Microstructure of SiC–TiC composite deposited at $TiCl_4/(TiCl_4 + SiCl_4) = 0.8$ for (a) SEM morphology; (b) polished topic view; (c) polished cross-section ($C_3H_8 = 25$ cm^3 min^{-1}, $H_2 = 3000$ cm^3 min^{-1} 1500°C and 100 torr).

where micro-twin or stacking fault exists. The magnified microstructure for the SiC–TiC interface in Fig. 10(b) shows that dislocations initiate from the interface and propagate parallel each other toward the TiC grain. A severe strain field contrasts is observed at the SiC–TiC interface owing to the residual stress induced by the mismatch of the coefficients of thermal expansion and elastic modulus between SiC and TiC. From stress calculation, the tensile stress is in TiC grain whereas the compressive stress is in SiC grain which deflects the crack resulting in toughness improvement.

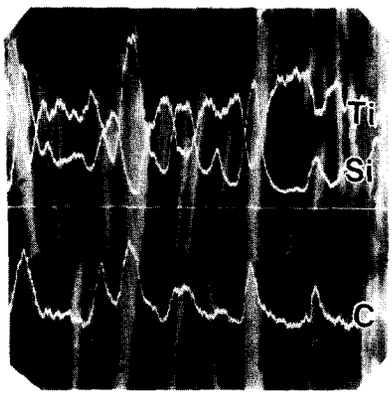

Fig. 9. Typical line scan profile of the SiC–TiC composite.

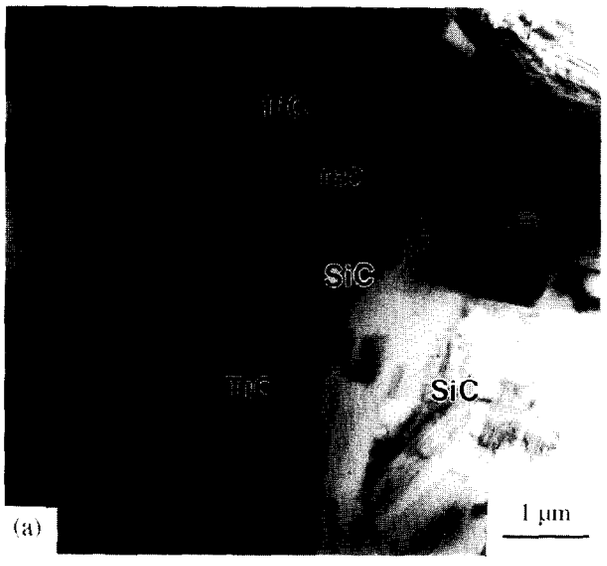

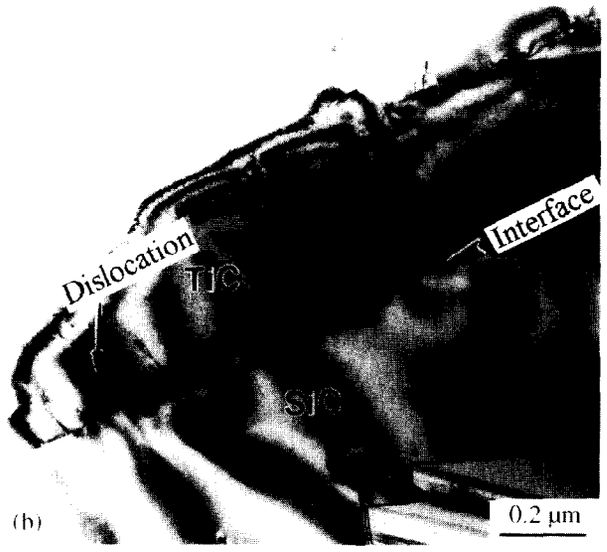

Fig. 10. Microstructure of the SiC–TiC composite observed by TEM for (a) bright field image; (b) SiC–TiC interface micrograph.

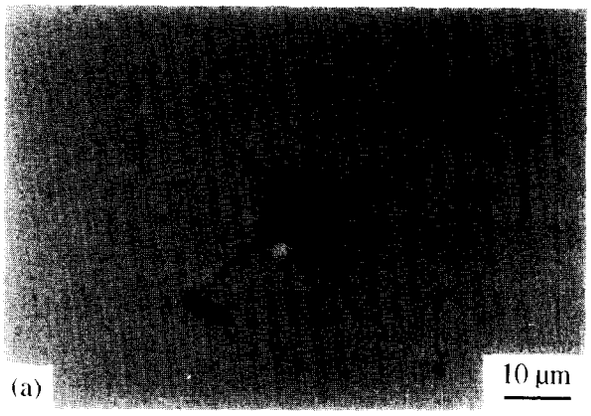

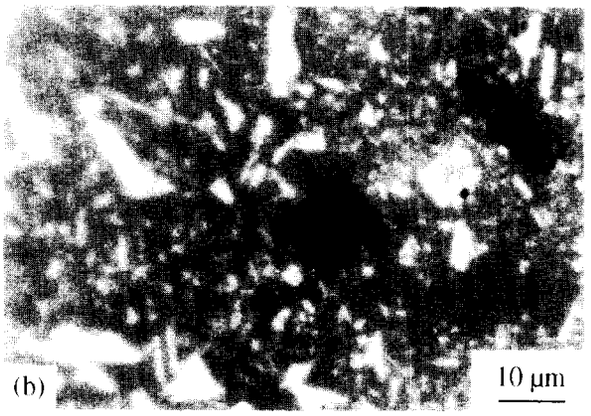

Fig. 11. Indentation crack propagation observed by OM for (a) a monolithic SiC; (b) SiC–TiC in-situ composite.

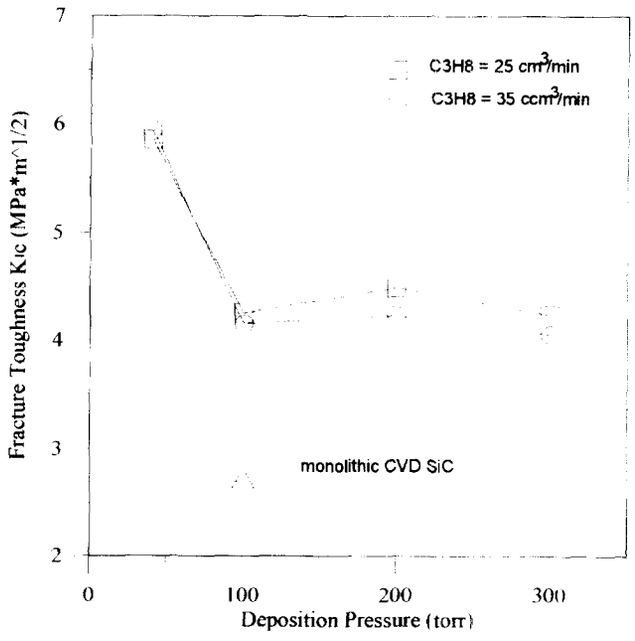

Fig. 12. Dependence of fracture toughness of SiC–TiC composite on deposition pressure for (□) $C_3H_8 = 25\,cm^3\,min^{-1}$; (○) $C_3H_8 = 35\,cm^3\,min^{-1}$.

3.2.1 Mechanical properties

The crack propagation by Vickers indentation shown in Fig. 11 is different for the CVD monolithic β-SiC and SiC–TiC in-situ composite. By incorporating TiC into SiC, the crack deflects considerably and consequently the propagation is inhibited due to the residual stress generated. Figure 12 shows the variation of fracture toughness

(K_{Ic}) with deposition pressure and C_3H_8 flow rate. The larger value of 5.9 MPa $m^{1/2}$ for K_{Ic} is obtained at 40 torr. This is roughly 2.2 times than for monolithic CVD SiC.

4 CONCLUSIONS

The CVD SiC–TiC in-situ composite deposited from a $SiCl_4$–$TiCl_4$–C_3H_8–H_2 system has been investigated. The results show that the morphologies change from facet to nodule depending on C_3H_8 flow rate. The SiC–TiC deposit is a dense plate without porosity and the growth rate is affected significantly by C_3H_8 inlet concentration with the maximum growth rate of 1.6 mm h^{-1}. TiC incorporates in the SiC matrix uniformly with dendrite structure, however the dendrite length decreases with increasing C_3H_8 concentration. No composition gradient occurs at the SiC–TiC interface. The maximum fracture toughness value is 5.9 MPa $m^{1/2}$ for the sample deposited at low pressure. The crack propagation in the composite is contrasted effectively by the TiC added. A severe strain field at the SiC–TiC interface has been observed by TEM.

REFERENCES

1. PREWO, K. M. & BRENNAN, J. J., High-strength silicon carbide fibre-reinforced glass-matrix composites. *J. Mater. Sci.*, **15** (1980) 463–468.
2. MARSHALL, D. B. & EVANS, A. G., Failure mechanisms in ceramic-fibre/ceramic-matrix composites. *J. Am. Ceram. Soc.*, **68** (1985) 225–231.
3. BECHER, P. F. & WEI, G. C., Toughening behavior in SiC-whisker-reinforced alumina. *J. Am. Ceram. Soc.*, **67** (1984) C267–269.
4. BECHER, P. F., HSUEH, C. H., ANGELINI, P. & TIEGS, T. N., Toughening behavior in whisker-reinforced ceramic matrix composites. *J. Am. Ceram. Soc.*, **71** (1988) 1050–1061.
5. LANGE, F. F., Effect of microstructure on strength of Si_3N_4-SiC composites system. *J. Am. Ceram. Soc.*, **56** (1973) 445–450.
6. ROBAYIE, J. A. L., KOPP, C. H. R. & HAUSNER, H., The influence of processing parameters on microstructure and mechanical properties of SiC–TiCp ceramics. *Ceram. Int.*, **21** (1995) 297–301.
7. NICKEL, J. J., SCHWEITZER, K. K. & LUXWNBERG, P., Gasphasenabscheidung im system Ti-Si-C. *J. Less-Common Metal*, **26** (1972) 335–353.
8. GOTO, T. & HIRAI, T., Microstructures of SiC–TiC in-situ composites prepared by chemical vapour deposition. *J. Japan Soc. Powder and Powder Metallurgy*, **34** (1987) 487–490.
9. GOTO, T. & HIRAI, T., Preparation of SiC–TiC *in-situ* composites by chemical vapor deposition. *Proc. Int. Conf. Chem. Vap. Deposition*, 10th, ed. G. W. Cullen. The Electrochemical Society, Inc. Pennington, NJ, 1987 pp. 1070–1079.
10. KAWAI, C., TERAKI, J., HIRANO, T. & NOMURA, T., Fabrication of a functionally gradient material of TiC–SiC system by chemical vapour deposition. *J. Ceram. Soc. Japan*, **100** (1992) 1117–1121.
11. KAWAI, C., SUZUKI, K. & TANAKA, K., Fracture toughness of TiC–SiC composites fabricated by CVD and the mechanism of toughening. *J. Ceram. Soc. Japan*, **100** (1992) 835–840.
12. TOUANEN, M., TEYSSANDIER, F., DUCARROIR, M., MALINE, M. & HILLEL, R., Microcomposite structures from chemical vapour deposition in the silicon-titanium-carbon system. *J. Am. Ceram. Soc.*, **76** (1993) 1473–1481.
13. TOUANEN, M., TEYSSANDIER, F. & DUCARROIR, M., Theoretical approach to chemical vapour deposition on the atomic system Ti-Si-C-Cl-H. *J. Mater. Sci. Lett.*, **8** (1989) 98–101.
14. STINTON, D. P. & LACKEY, W. J., Simultaneous chemical vapour deposition of SiC-dispersed phase composites. *Ceram. Eng. Sci. Proc.*, **6** (1985) 707–715.
15. PARRETTA, A., CAMANZI, A., GIUNTA, G. & MAZZARANO, A., Morphological aspects of silicon carbide chemically vapour-deposited on graphite. *J. Mater. Sci.*, **26** (1991) 6057.
16. NIIHARA, K., NAKAHIRA, A. & HIRAI, T., The effect of stoichiometry on mechanical properties of boron carbide. *J. Am. Ceram. Soc.*, **67** (1984) C13.